CrossMark

ORIGINAL ARTICLE

Furan and Julolidine-Based "Turn-on" Fluorescence Chemosensor for Detection of F⁻ in a Near-Perfect Aqueous Solution

Ha Young Jeong[1] · Seong Youl Lee[1] · Cheal Kim[1]

Abstract A new fluorescent sensor **1**, containing furan and julolidine moieties linked through a Schiff-base, has been synthesized. Distinct "turn-on" fluorescence enhancement of **1** was observed upon the addition of F⁻ in a near-perfect aqueous solution. The binding capabilities of **1** with F⁻ were studied by using fluorescent spectroscopic techniques, ESI-mass analysis and NMR titration measurements. The detection limit for the analysis of F⁻ was found to be 10.02 μM, which is below the WHO guideline (79 μM) for drinking water. Practically, the sensing ability of **1** for F⁻ was successfully applied in real water samples. The sensing mechanism for F⁻ was proposed to be the ICT mechanism via the hydrogen bonding, which was well explained by theoretical calculations.

Keywords Fluoride · Fluorometric · Furan · Julolidine · Theoretical calculations

Introduction

To the design and development of chemosensor for detecting target anions have been paid much attention, due to their important roles in a wide range of chemical, biological, medical and environmental processes [1–6]. Among various anions, the smallest anion F⁻ with a high charge density is of special attention due to its role in dental and osteoporosis treatments [7, 8]. Proper intake of fluoride helps to prevent tooth loss and demineralization of tooth enamel, but its high concentration or ingestion of even low concentration for a prolong period causes skeletal fluorosis, depression of thyroid activity, bone disorders and adverse effect on the immune system [9–13]. The World Health Organization (WHO) has set 79 μM as the maximum contaminant level of fluoride in drinking water [14]. Therefore, it is of importance to develop a chemosensor for highly sensitive detection of fluoride [15–22].

Several conventional methods such as inductively coupled-plasma atomic emission spectrometry, atomic absorption spectroscopy, and electrochemical methods, have been applied to detect various anions [23–25]. However, most of these methods require sophisticated equipment, tedious sample preparation procedures, and trained operators. In contrast, fluorometric methods are especially attractive because of their advantages, such as low cost, facile sample preparation, the simplicity and high sensitivity. Therefore, the fluorescent signaling methods have been widely applied in biology and environment [26–36].

Furan moieties have been widely used as a fluorescence signaling agent [37–39], and juloilidine is a well-known chromophore with a hydrophilic character and acts as an electron donor site [40, 41]. In addition, Schiff-bases have been widely used in development of chemosensors toward various anions. In particular, Schiff bases containing phenolic groups are known to be efficient sensors for anions, because the phenol group can interact with anions through hydrogen bonding [42–45]. Therefore, we expected that the chemosensor having the furan and julolidine moieties linked with Schiff-base would show a unique fluorescent property toward a specific anion.

Herein, we report a chemosensor **1** based on one-step condensation of julolidine and furan moieties connected via Schiff-base. Sensor **1** showed a turn-on fluorescence in the presence of

✉ Cheal Kim
chealkim@seoultech.ac.kr

[1] Department of Fine Chemistry and Department of Interdisciplinary Bio IT Materials, Seoul National University of Science and Technology, Seoul 139-743, South Korea

F⁻ in a near-perfect aqueous solution. The sensing mechanism of **1** toward F⁻ was proposed to be the ICT mechanism via hydrogen bonding, which was well explained by theoretical calculations.
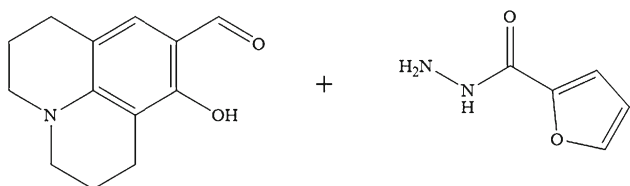
Experimental

Materials and Equipment

All the solvents and reagents (analytical grade and spectroscopic grade) were obtained from Sigma-Aldrich and used as received. ^{1}H NMR and ^{13}C NMR measurements were performed on a Varian 400 MHz and 100 MHz spectrometer, and chemical shifts were recorded in ppm. Electrospray ionization mass spectra (ESI-MS) were collected on a Thermo Finnigan (San Jose, CA, USA) LCQTM Advantage MAX quadrupole ion trap instrument. Absorption spectra were recorded at room temperature using a Perkin Elmer model Lambda 25 UV/Vis spectrometer. The emission spectra were recorded on a Perkin-Elmer LS45 fluorescence spectrometer. Elemental analysis for carbon, nitrogen and hydrogen was carried out by using a Vario micro cube elemental analyzer (ELEMENTAR) in laboratory center of Seoul National University of Science and Technology, Korea. FT-IR spectrum was collected on an Agilent Cary 670 FTIR spectrometer.

Synthesis of Sensor 1

Sensor **1** was prepared by the reaction of 8-hydroxyjulolidine-9-carboxaldehyde (0.22 μL, 1.0 mmol) and furan-2-carbohydrazide (0.13 g, 1.0 mmol) in ethanol. Two drops of HCl were added into the reaction solution, which was stirred for 2 days at room temperature. A yellow precipitate was filtered, washed several times with cold ethanol, and dried in vacuum. Yield: 0.29 g (89%). The ^{1}H NMR spectra were recorded in DMSO-d_6, and the descriptions of the signals include: s = singlet, d = doublet, t = triplet and m = multiplet (400 MHz, 25 °C): δ = 11.82 (s, 1H), 11.66 (s, 1H), 8.29 (s, 1H), 7.91 (d, 1H), 7.22 (d, 1H), 6.68 (d, 2H), 3.16 (m, 4H), 2.48 (m, 4H), 1.84 (m, 4H); ^{13}C NMR (100 MHz, CD$_3$CN, 25 °C): δ = 154.91, 153.72, 151.35, 145.75, 128.56, 115.23, 112.31, 106.07, 49.61, 26.82, 21.23. IR (KBr, ν cm^{-1}) = 3209 (m), 2938 (m), 2839 (m), 2361 (m), 2160 (m), 1627 (m), 1590 (s), 1507 (s), 1461 (m), 1349 (m), 1292 (s), 1174 (s), 1086 (m), 1013 (m), 968 (m), 844 (m), 744 (s), 662 (s). Anal. calcd for C$_{18}$H$_{19}$N$_3$O$_3$: C, 66.45; H, 5.89; N, 12.91%. Found: C, 66.27; H, 5.94; N, 12.83%.

Fluorescence Titration

A stock solution (5 mM) of sensor **1** was prepared in DMSO and 6 μL of the sensor **1** (5 mM) was diluted to 2.994 mL bis-tris buffer solution to make final concentration of 10 μM. Then, 3–72 μL of the stock solution of tetraethylammonium fluoride (TEAF, 100 mM) were added to **1** solution (10 μM). After mixing them for a few seconds, fluorescence spectra were taken at room temperature.

UV-vis Titration

A stock solution (5 mM) of sensor **1** was prepared in DMSO and 6 μL of the sensor **1** (5 mM) was diluted to 2.994 mL bis-tris to make final concentration of 10 μM. Then, 3–39 μL of the stock solution of TEAF (100 mM) were added to **1** solution (10 μM). After mixing them for a few seconds, UV-vis spectra were taken at room temperature.
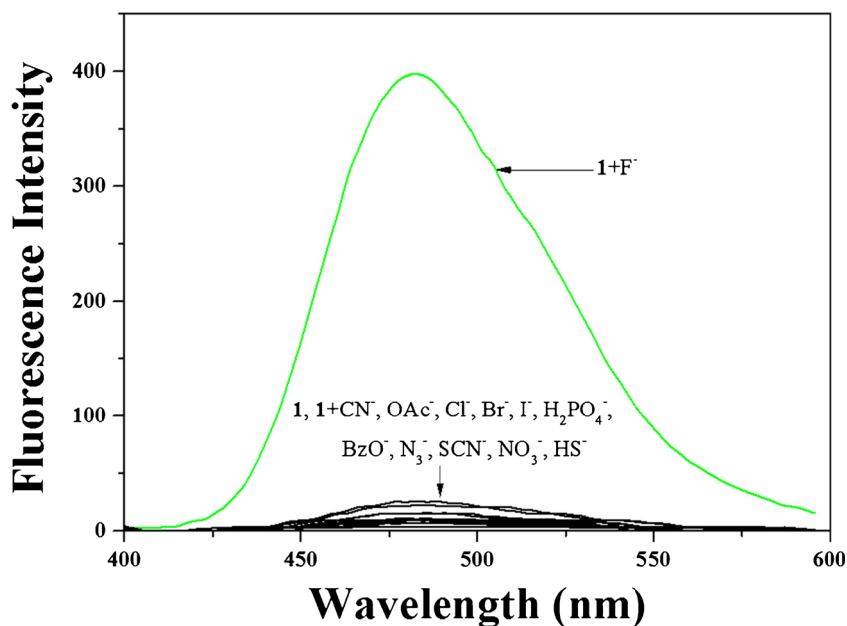
Job Plot Measurement

A series of solutions containing sensor **1** (70 μM) and TEAF (70 μM) were prepared in such a manner that the total volumes of sensor **1** and anion remained constant (3 mL), and bis-tris buffer was used as a solvent. After mixing them for a few seconds, UV-vis spectra were taken at room temperature. Job plot was drawn by plotted against the molar fraction of sensor **1** under the constant total concentration.

Competition Experiment

A stock solution of sensor **1** (5 mM) was prepared in DMSO and 6.0 μL of this solution was diluted to 2.994 mL of bis-tris buffer to make final concentration of 10 μM. Stock solutions (100 mM) of various anions such as CN⁻, Cl⁻, Br⁻, I⁻, H$_2$PO$_4$⁻, BzO⁻, OAc⁻, SCN⁻, N$_3$⁻, NO$_2$⁻ and HS⁻ were prepared and 63 μL of each anion solution was taken and added to 3 mL of the solution of sensor **1** (10 μM) to give 210 equiv. of anions. Then, 63 μL of F⁻ solution (100 mM) was added

Scheme 1 Synthesis of **1**

into the mixed solution of each anion and **1** to make 210 equiv. After mixing them for a few seconds, fluorescence spectra were taken at room temperature.

pH Effect Test

A series of buffers with pH values ranging from 2 to 12 were prepared by mixing sodium hydroxide solution and hydrochloric acid in bis-tris buffer. After the solution with a desired pH was achieved, a stock solution (5 mM) of sensor **1** was prepared in DMSO and 6.0 μL of this solution was diluted to 3 mL of bis-tris buffer to make final concentration of 10 μM. Stock solutions (100 mM) of F^- were prepared at different pH

and 63 μL of each stock solution was taken and added to the each pH solution (2–12) of sensor **1** (5 μM) to give 210 equiv. of anions. After stirring them for a few seconds, fluorescence spectra were taken at room temperature.

^{1}H NMR Titration

Four NMR tubes of sensor **1** (1.62 mg, 0.005 mmol) dissolved in DMSO-d_6 (700 μL) were prepared and then four different concentrations (0, 0.0025, 0.005 and 0.025 mmol) of TEAF dissolved in DMSO-d_6 were added to each solution of sensor **1**. After shaking them for 1 min, ^{1}H NMR spectra were obtained at room temperature.
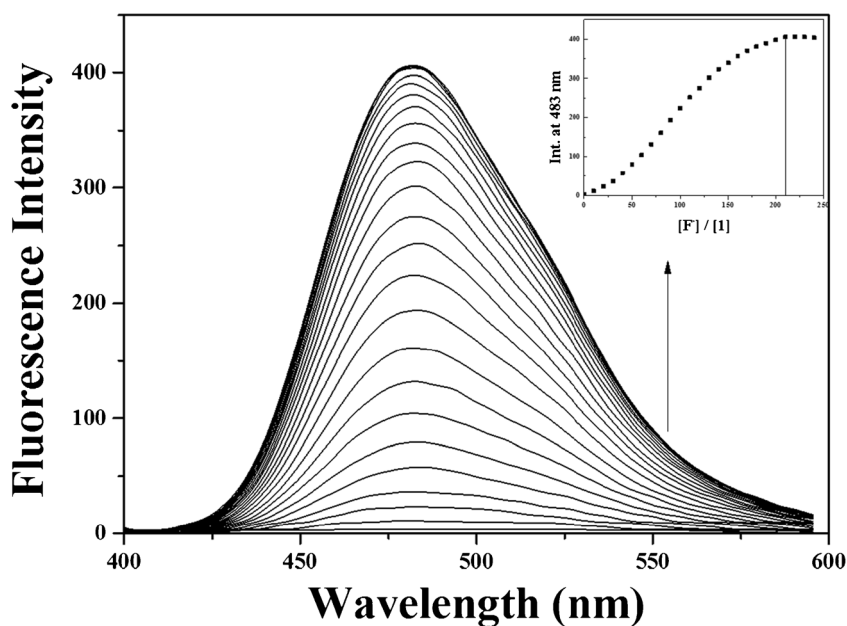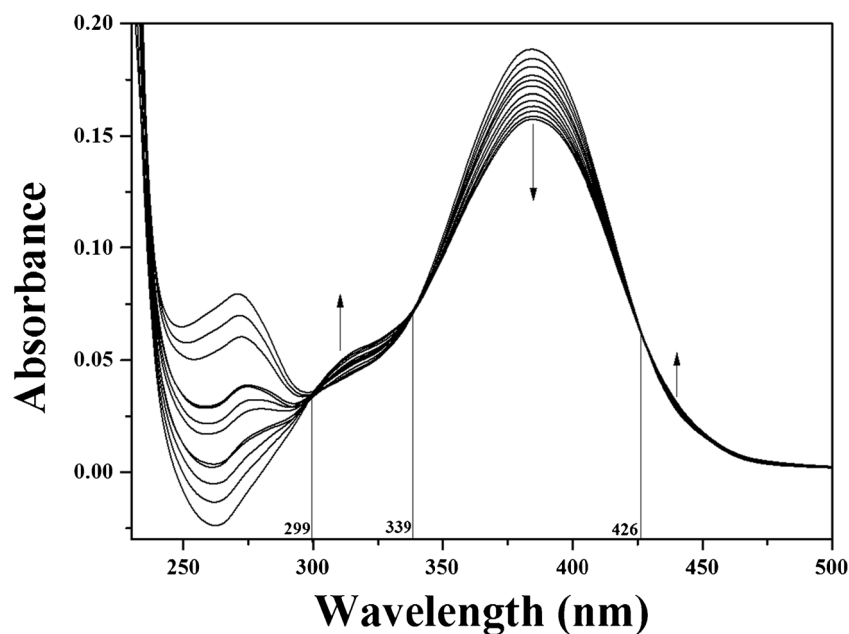
Fig. 3 Absorption spectral changes of **1** (10 μM) in the presence of different concentrations of F⁻ in bis-tris buffer at room temperature

Theoretical Calculation Methods

All DFT/TDDFT calculations based on the hybrid exchange correlation functional B3LYP [46, 47] were carried out using Gaussian 03 program [48]. The 6-31G** basis set [49, 50] was used for the main group elements. In vibrational frequency calculations, there was no imaginary frequency for the optimized geometries of **1** and **1**-F⁻, suggesting that these geometries represented local minima. For all calculations, the solvent effect of water was considered by using the Cossi and Barone's CPCM (conductor-like polarizable continuum model) [51, 52]. To investigate the electronic properties of singlet excited states, time-dependent DFT (TDDFT) was performed in the ground state geometries of **1** and **1**-F⁻. The 25 singlet-singlet excitations were calculated and analyzed. The GaussSum 2.1 [53] was used to calculate the contributions of molecular orbitals in electronic transitions.

Results and Discussion

Sensor **1** was synthesized by direct condensation of 8-hydroxyjulolidine-9-carboxaldehyde and furan-2-carbohydrazide with 89% yield in ethanol (Scheme 1), and characterized by ¹H NMR, ¹³C NMR, FT-IR spectrometry and elemental analyses.

Fluorescence Studies of 1 toward F⁻

To study the sensing ability, sensor **1** was treated with various anions such as CN⁻, F⁻, Cl⁻, Br⁻, I⁻, $H_2PO_4^-$, BzO⁻, OAc⁻, SCN⁻, N_3^-, NO_2^- and HS⁻ in bis-tris buffer (10 mM, pH 7.0). Compared to the other anions examined, the prominent fluorescence change of **1** was observed in the presence of F⁻ with a visual color change from colorless to green (Fig. 1). In contrast, sensor **1** showed no or weak fluorescence with other anions. The fluorescence titration experiments were performed by
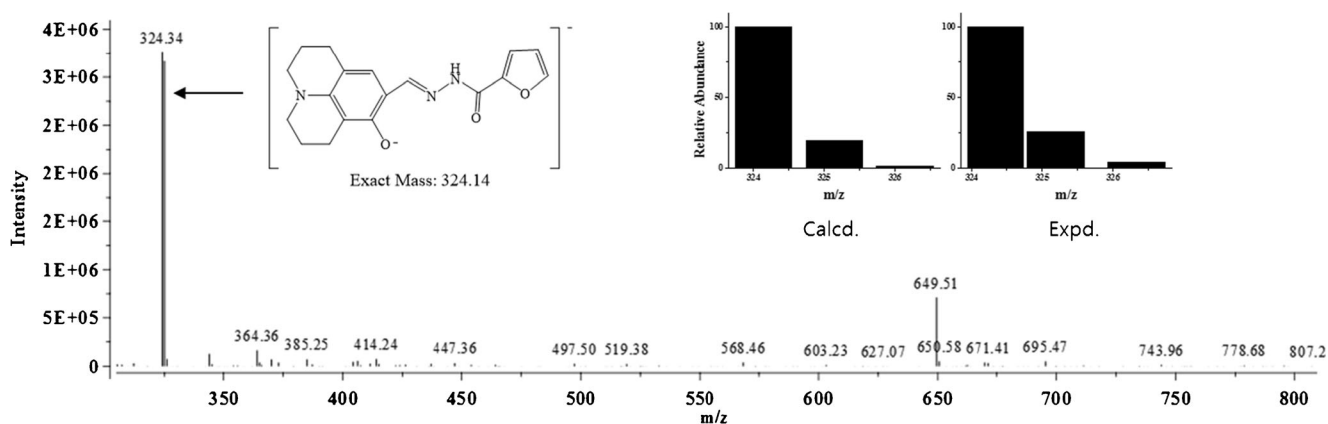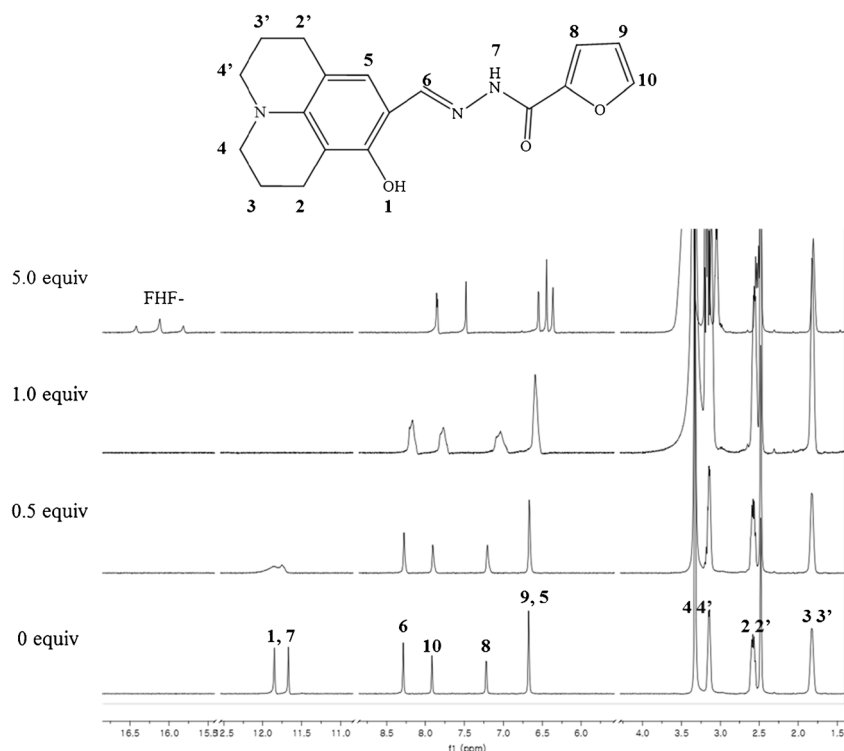

Fig. 4 Negative-ion electrospray ionization mass spectrum of **1** (100 μM) upon addition of TEAF (1.0 equiv)

Fig. 5 ^{1}H NMR titration of **1** with F$^-$

increasing concentration of F$^-$ into a solution of **1**. As shown in Fig. 2, the fluorescence intensity at 483 nm increased about 400 folds ($\lambda_{ex} = 384$ nm). The corresponding UV-vis spectral changes were also investigated (Fig. 3). The UV-vis titration of **1** with F$^-$ solution revealed that the absorption bands at 250 nm and 375 nm decreased, and new bands at 325 nm and 450 nm increased slightly. Clear isosbestic points emerged at 299 nm, 339 nm and 426 nm during the UV-vis titration,

which indicated that the only one species was formed between **1** and F$^-$.

The stoichiometry of **1** with F$^-$ was determined by Job plot analysis using emission titration experiments in the presence of various molar fractions of F$^-$ [54]. The Job plot for the binding between **1** and F$^-$ exhibited a 1:1 stoichiometry (Fig. S1). In addition, the formation of the 1:1 species between **1** and F$^-$ was further confirmed by the appearance of a peak at
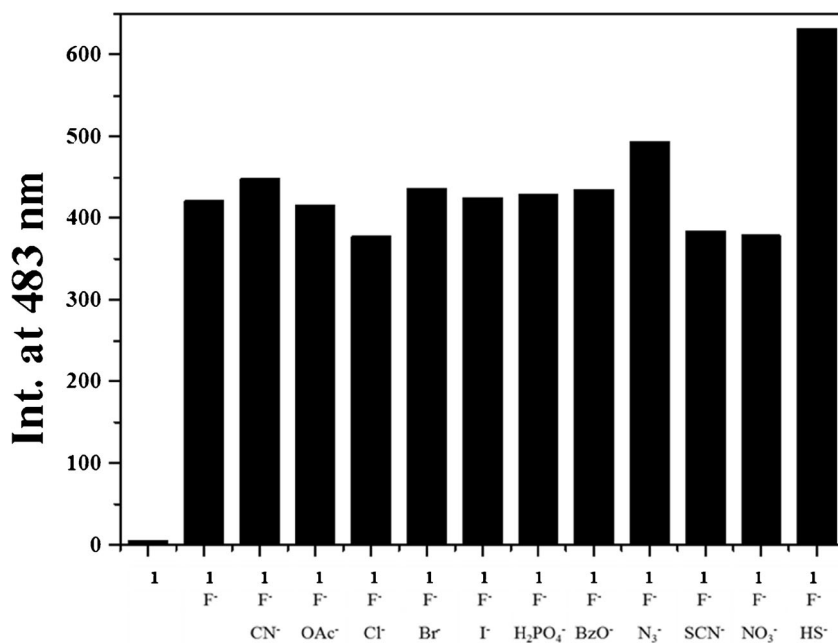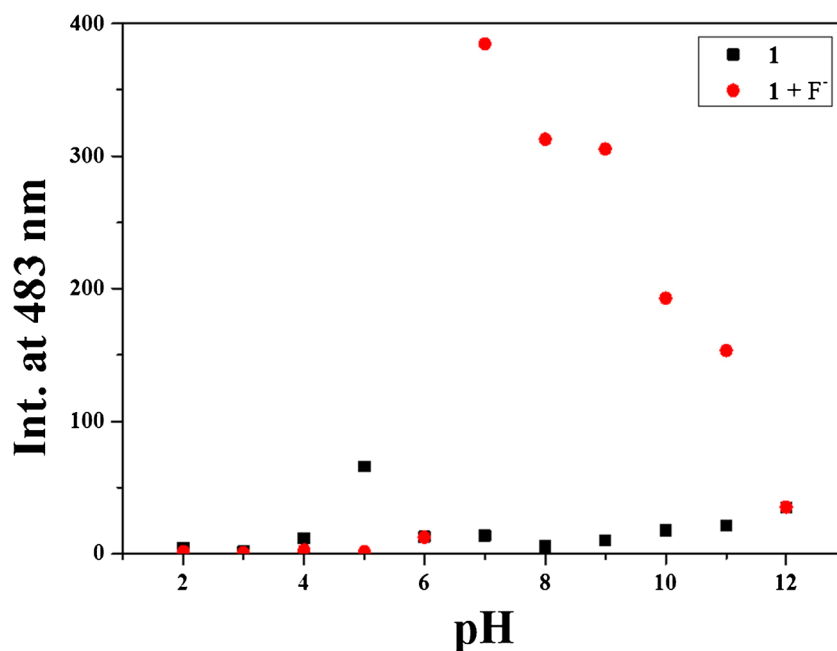
Fig. 6 Competitive selectivity of **1** (10 μM) toward F$^-$ (210 equiv) in the presence of other anions (210 equiv)

Fig. 7 Fluorescence spectra (483 nm) of **1** (10 μM) and **1**-F⁻, respectively, at pH 2–12 in bis-tris buffer at room temperature

m/z 324.34, assignable to [**1** - H⁺]⁻ (calcd: 324.14) in the ESI-mass analysis (Fig. 4). The evidence for the reaction between **1** and F⁻ was further provided by ^{1}H NMR titration (Fig. 5). Upon the addition of 1.0 equiv. of F⁻, the signals of -OH- and -NH- completely disappeared, which may be ascribed to the strong hydrogen bonding interaction between F⁻ and the -OH- and -NH- units of **1**. On excess addition of F⁻ (5.0 equiv) to **1** solution, a new peak at 16.11 ppm appeared, indicating the formation of FHF⁻ species. At the same time, most of aromatic protons were shifted to upfield, which indicates that the negative charge generated from deprotonation of **1** by F⁻ might be delocalized through the whole molecule. There was no shift in the position of the proton signals on further addition of F⁻ (>5.0 equiv).
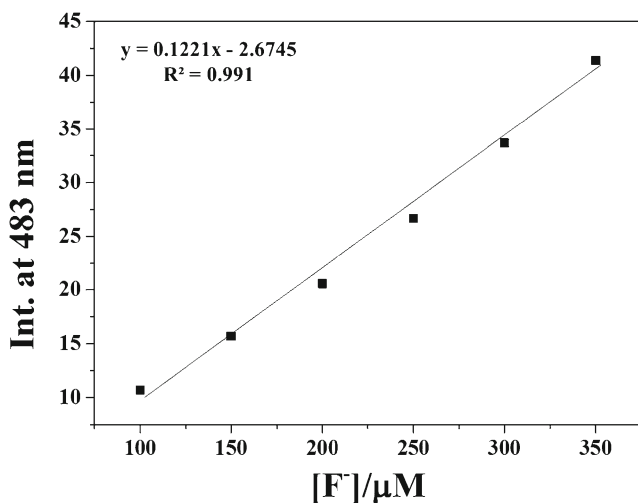
The association constant was calculated to be 7.5×10^2 M⁻¹ from a Benesi-Hildebrand plot using emission changes at 483 nm (Fig. S2) [55]. This value is within the range of those (10^1–10^6) reported for F⁻ sensors. The detection limit (DL) of sensor **1** for F⁻ detection was determined from a plot of fluorescence intensity as a function of F⁻ concentration (Fig. S3) [56]. The DL was found to be 10.02 μM, which is lower than the maximum allowable level (79 μM) of F⁻ regulated by WHO in drinking water.

To further examine the fluorescence response of sensor **1** toward F⁻ in the presence of preferentially competing species, competition experiments with various anions were conducted (Fig. 6). Upon addition of 210 equiv. of F⁻ in the presence of other anions (210 equiv), such as CN⁻, OAc⁻, Cl⁻, Br⁻, I⁻, $H_2PO_4^-$, BzO⁻, N_3^-, SCN⁻, NO_2^- and HS⁻, there was no interference in the detection of F⁻ from other anions.

In order to apply to the environmental systems, the pH dependence of **1** in the absence and presence of F⁻ was conducted at various pH (Fig. 7). The increase of intensity caused by addition of F⁻ was observed between pH 7.0 and 11.0. This

Fig. 8 Emission intensity (483 nm) of 1 as a function of F⁻ concentration. [**1**] = 10 μmol/L and [F⁻] = 100–350 μmol/L in bis-tris buffer

y = 0.1221x - 2.6745
R² = 0.991

Table 1 Determination of F⁻ in water samples [a]

Sample	F⁻ added (μmol/L)	F⁻ found (μmol/L)	Recovery (%)	R.S.D. (n = 3) (%)
Drinking water	0.0	0.0		1.22
	100	98.97	98.97	2.46
Tap water	0.0	48.67		1.26
	100	150.81	101.44	3.43

[a] Conditions: [**1**] = 10 μmol L⁻¹ in 10 mM bis-tris buffer solution (pH 7.0)

Fig. 9 The energy-minimized structures of (a) **1** and (b) **1**-F⁻

Dihedral angle (1C, 2C, 3N, 4C) : -3.946°

F-6H : 1.4678 Å
F-7H : 1.6962 Å
5O-6H : 1.0398 Å
3N-7H : 1.0454 Å

Dihedral angle (1C, 2C, 3N, 4C) : 54.427°
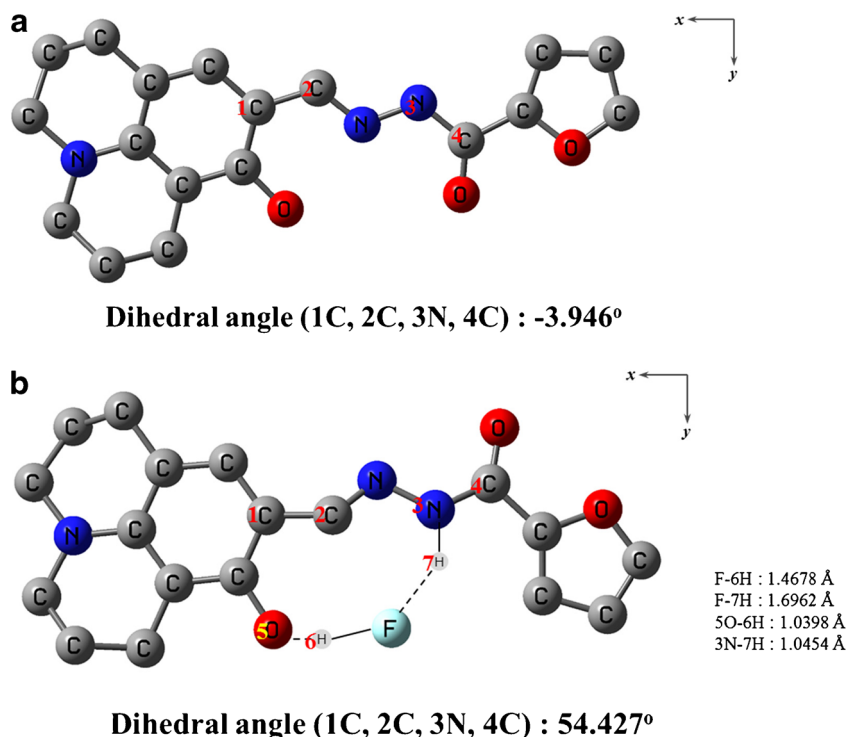
result warranted its application under physiological conditions, without any change in detection F⁻.

For practical application, we constructed a calibration curve for the determination of F⁻ by **1** (Fig. 8). A good linear relationship was observed for **1**-F⁻ species with a correlation coefficient of $R^2 = 0.991$ ($n = 3$). To evaluate the practical abilities of **1** with F⁻, drinking and tap water samples were selected and each sample was analyzed with three replicates. As shown in Table 1, satisfactory recoveries and suitable R.S.D. values for F⁻ were obtained. These results suggested that chemosensor **1** could be useful for the measurements of F⁻ in chemical and environmental applications.
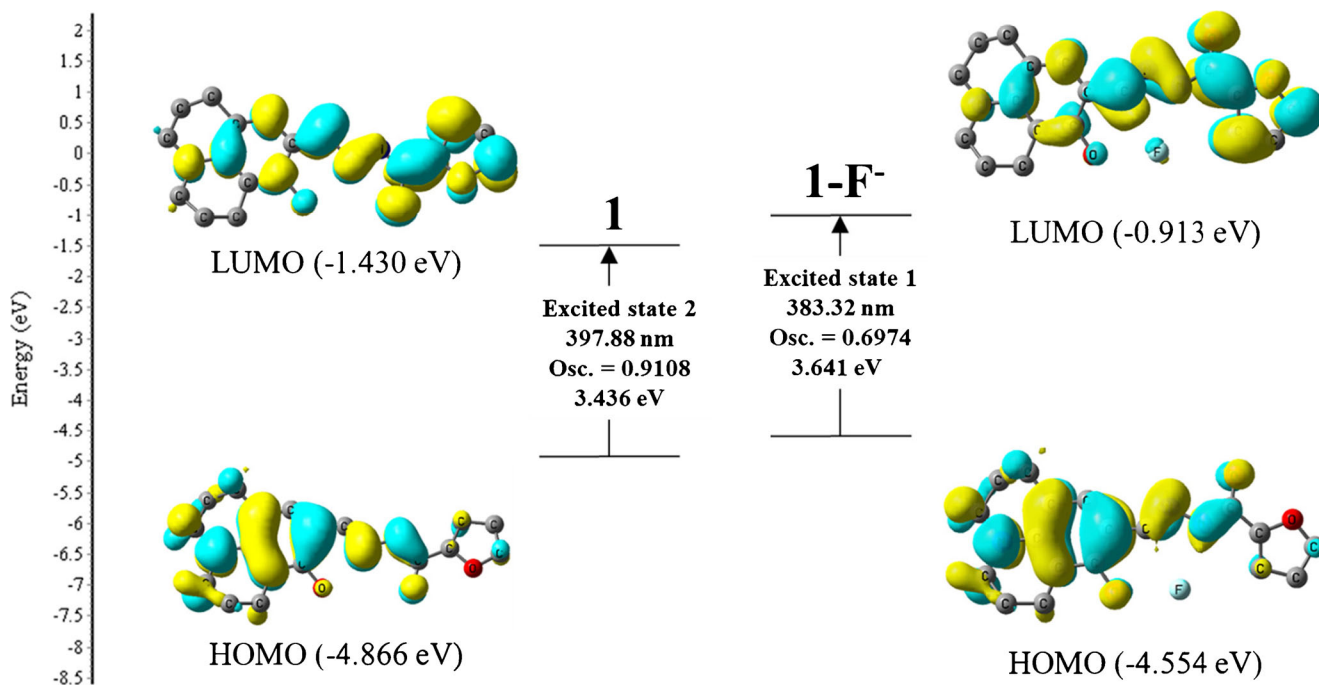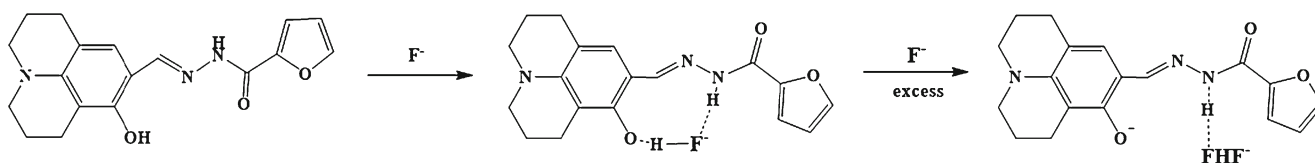

Fig. 10 Molecular orbital diagrams and excitation energies of **1** and **1**-F⁻

Scheme 2 Proposed sensing mechanism of fluoride by **1**

Theoretical Studies

In order to understand fluorescence sensing mechanism of **1** to F$^-$, electronic properties were calculated by using the Gaussian 03 program. The density functional theory (DFT) and time dependent-density functional theory (TD-DFT) calculations were conducted with the B3LYP/6-31G(d, p) method basis set. To evaluate the solvent effect, water was used as a solvent by using the CPCM method. The optimized geometry structures of **1** and **1**-F$^-$ species are shown in Fig. 9. The energy-minimized structure of **1** showed a nearly planar structure with the dihedral angle of 1C, 2C, 3 N, 4C = −3.946^o (Fig. 9a). For **1**-F$^-$, F$^-$ hydrogen bonded with 6H and 7H of **1** with dihedral angle of 1C, 2C, 3 N, 4C = 54.427 ^{o} (Fig. 9b). The transition energies and oscillator strengths of **1** and **1**-F$^-$ were obtained from TD-SCF calculation. In the case of **1**, the main molecular orbital (MO) contribution of the 2nd lowest excited state was determined for the HOMO → LUMO transition (397.88 nm, Fig. S4). The HOMO orbital mainly lied in the julolidine moiety, and the LUMO orbital did in the furan one. These results indicated ICT from the julolidine to the furan. For **1**-F$^-$, the 1st excited state was found to be relevant to the 'turn-on' fluorescence showing predominant ICT band (383.32 nm, Fig. S5). The HOMO was localized in electron-donor parts of the julolidine moiety, while the LUMO was located in electron-acceptor sites of the furan one. These transitions indicated the ICT band from the julolidine to the furan. MO diagrams and excitation energies of **1** and **1**-F$^-$ are shown in Fig. 10. Thus, these results suggested that the "turn-on" sensing mechanism of **1** toward F$^-$ may be due to the ICT process. Based on Job plot, ^{1}H NMR titration and theoretical calculations, the sensing mechanism of F$^-$ by **1** is depicted in Scheme 2.

Conclusion

We have successfully synthesized and characterized a new chemosensor **1** for selective detection of F$^-$ in a near-perfect aqueous solution. The binding properties of the sensor **1** toward F$^-$ have been studied by spectroscopic techniques, ESI-mass analysis and ^{1}H NMR titration. Sensor **1** showed high sensitivity to F$^-$ with a detection limit of 10.02 μM and excellent selectivity avoiding the interference from other anions. The sensing mechanism for F$^-$ was proposed to be the ICT mechanism via hydrogen bonding with DFT and TD-DFT

studies. For practical application, **1** could be used to detect and quantify F$^-$ levels in real water samples.

References

1. Mizukami S, Nagano T, Urano Y, Odani A, Kikuchi K (2002) A fluorescent anion sensor that works in neutral aqueous solution for bioanalytical application. J Am Chem Soc 124:3920–3925
2. Beer PD, Gale PA (2001) Anion recognition and sensing: the state of the art and future perspectives. Angew Chem Int Ed 40:486–516
3. Santos-Figueroa LE, Moragues ME, Climent E, Agostini A, Martinez-Manez R, Sancenon F (2013) Chromogenic and fluorogenic chemosensors and reagents for anions. A comprehensive review of the years 2010–2011. Chem Soc Rev 42:3489–3613
4. Lee SA, You GR, Choi YW, Jo HY, Kim AR, Noh I, Kim S-J, Kim Y, Kim C (2014) A new multifunctional Schiff base as a fluorescence sensor for Al^{3+} and a colorimetric sensor for CN$^-$ in aqueous media: an application to bioimaging. Dalton Trans 43:6650–6659
5. Song EJ, Kim H, Hwang IH, Kim KB, Kim AR, Noh I, Kim C (2014) A single fluorescent chemosensor for multiple target ions: recognition of Zn^{2+} in 100% aqueous solution and F- in organic solvent. Sensors Actuators B Chem 195:36–43
6. Park GJ, Hwang IH, Song EJ, Kim H, Kim C (2014) A colorimetric and fluorescent sensor for sequential detection of copper ion and cyanide. Tetrahedron 70:2822–2828
7. Zhou Z, Wang Q, Tan C (2014) Soft matter anion sensing based on lanthanide (Eu^{3+} and TB^{3+}) luminescent hydrogels. Soft Mater 12:98–102
8. Ji X, Yao Y, Li J, Yan X, Huang F (2013) A supramolecular cross-linked conjugated polymer network for multiple fluorescent sensing. J Am Chem Soc 135:74–77
9. Caballero A, Zapata F, Beer PD (2013) Interlocked host molecules for anion recognition and sensing. Coord Chem Rev 257:2434–2455
10. Rostami A, Taylor MS (2012) Polymers for anion recognition and sensing. Macromol Rapid Commun 33:21–34
11. Browne D, Whelton H, O'Mullane D (2005) Fluoride metabolism and fluorosis. J Dent 33:177–186
12. Schwarzenbach RP, Escher BI, Fenner K, Hofstetter TB, Johnson CA, Guten U, Werli B (2006) The challenge of micropollutants in aquatic systems. Science 313:1072–1077
13. Jagtap S, Yenkie MK, Labhsetwar N, Rayalu S (2012) Fluoride in drinking water and Defluoridation of water. Chem Rev 112:2454–2466

14. Graham N (1999) Guidelines for drinking-water quality, 2nd edition, addendum to volume 1 – recommendations, World Health Organisation, Geneva, 1998, 36 pages. Urban Water 1:183

15. Ryu HH, Lee YJ, Kim SE, Jo TG, Kim C (2016) A colorimetric F^- chemosensor with high selectivity: experimental and theoretical studies. J Incl Phenom Macrocycl Chem 86:111–119

16. Lee JH, Lee SH, So YA, Park GJ, Kim C (2015) Simultaneous detection of F^- and CN^- by a simple colorimetric Chemosensor with high selectivity. Bull Kor Chem Soc 36:1618–1624

17. Lee HJ, Park SJ, Sin HJ, Na YJ, Kim C (2015) A selective colorimetric chemosensor with an electron-withdrawing group for multi-analytes CN^- and F^-. New J Chem 39:3900–3907

18. Lee M, Jo S, Lee D, Xu Z, Yoon J (2015) A new naphthalimide derivative as a selective fluorescent and colorimetric sensor for fluoride, cyanide and CO_2. Dyes Pigments 120:288–292

19. Cho J, Kim I, Moon JH, Jung HS, Kim JS (2016) Triazolium-promoted highly selective fluorescence "turn-on" detection of fluoride ions. Dyes Pigments 132:248–254

20. Park JJ, Kim Y-H, Kim C, Kang J (2011) Naked eye detection of fluoride and pyrophosphate with an anion receptor utilizing anthracene and nitrophenyl group as signaling group. Tetrahedron Lett 52:2759–2763

21. Kang J, Lee YJ, Lee SK, Park JJ, Kim Y, Kim SJ, Kim C (2010) A naked-eye detection of fluoride with urea/thiourea receptors which have both a benzophenone group and a nitrophenyl group as a signalling group. Supramol Chem 22:267–273

22. Yoo M, Park S, Kim H-J (2016) Activatable colorimetric and fluorogenic probe for fluoride detection by oxazoloindole-to-hydroxyethylindolium transformation. RSC Adv 6:19910–19915

23. Rao KS, Balaji T, Rao TP, Babu Y, Naidu GRK (2002) Determination of iron, cobalt, nickel, manganese, zinc, copper, cadmium and lead in human hair by inductively coupled plasma-atomic emission spectrometry. Spectrochim Acta Part B-atomic Spectrosc 57:1333–1338

24. Sturgeon RE, Berman SS, Desaulniers A, Russell DS (1979) Determination of iron, manganese, and zinc in seawater by graphite furnace atomic absorption spectrometry. Anal Chem 51:2364–2369

25. Gulaboski R, Mireski V, Scholz F (2002) An electrochemical method for determination of the standard Gibbs energy of anion transfer between water and n-octanol. Electrochem Commun 4:277–283

26. Montoya LA, Pluth MD (2012) ChemComm selective turn-on fluorescent probes for imaging hydrogen sulfide in living cells w. 4767-4769

27. Park GJ, Jo HY, Ryu KY, Kim C (2014) A new coumarin-based chromogenic chemosensor for the detection of dual analytes al^{3+} and F^-. RSC Adv 4:63882–63890

28. Sen B, Mukherjee M, Banerjee S, Chattopadhyay P (2015) A rhodamine-based "turn-on" al^{3+} ion-selective reporter and the resultant complex as a secondary sensor for F^- ion are applicable to living cell staining. Dalton Trans 44:8708–8717

29. Datta BK, Thiyagarajan D, Ramesh A, Das G (2015) A sole multi-analyte receptor responds with three distinct fluorescence signals: traffic signal like sensing of Al^{3+}, Zn^{2+} and F^-. Dalton Trans 44:13093–13099

30. Ghosh K, Panja S, Sarkar T (2015) Rhodamine-linked pyridyl thiourea as a receptor for selective recognition of F^-, Al^{3+} and ag^+ under different conditions. Supramol Chem 27:490–500

31. Kim YS, Lee JJ, Choi YW, Kim C (2016) Simultaneous bioimaging recognition of cation Al^{3+} and anion F^- by a fluorogenic method. Dyes Pigments 129:43–53

32. Liu H, Zhang B, Tan C, Jiang Y (2016) Simultaneous bioimaging recognition of Al^{3+} and Cu^{2+} in living-cell, and further detection of F^- and S^{2-} by a simple fluorogenic benzimidazole-based chemosensor. Talanta 161:309–319

33. Lee JJ, Park GJ, Kim YS, Lee SY, Lee HJ, Noh I, Kim C (2015) A water-soluble carboxylic-functionalized chemosensor for detecting Al^{3+} in aqueous media and living cells: experimental and theoretical studies. Biosens Bioelectron 69:226–229

34. Choi YW, Park GJ, Na YJ, Jo HY, Lee SA, You GR, Kim C (2014) A single schiff base molecule for recognizing multiple metal ions: a fluorescence sensor for Zn(II) and al(III) and colorimetric sensor for Fe(II) and Fe(III). Sensors Actuators B Chem 194:343–352

35. Jang YK, Nam UC, Kwon HL, Hwang IH, Kim C (2013) A selective colorimetric and fluorescent chemosensor based-on naphthol for detection of Al^{3+} and Cu^{2+}. Dyes Pigments 99:6–13

36. Kim KB, Kim H, Song EJ, Kim S, Noh I, Kim C (2013) A cap-type Schiff base acting as a fluorescence sensor for zinc(II) and a colorimetric sensor for iron(II), copper(II), and zinc(II) in aqueous media. Dalton Trans 42:16569–16577

37. Yang C, Gong D, Wang X, Deng Y, Guo Y (2016) A new highly copper-selective fluorescence enhancement chemosensor based on BODIPY excitable with visible light and its imaging in living cells. Sensors Actuators B Chem 224:110–117

38. Boonkitpatarakul K, Wang J, Niamnont N, Mcdonald L, Pang Y, Sukwattanasinitt M (2016) Novel turn-on fluorescent sensors with mega stokes shifts for dual detection of Al^{3+} and Zn^{2+}. ACS Sensors 1:144–150

39. Hu Y, Ke Q, Yan C, Huang XH, Hu S (2016) A new fluorescence chemosensor for selective detection of copper ion in aqueous solution. Tetrahedron Lett 57:2239–2243

40. Choi YW, You GR, Lee JJ, Kim C (2016) Turn-on fluorescent chemosensor for selective detection of Zn^{2+} in an aqueous solution: experimental and theoretical studies. Inorg Chem Commun 63:35–38

41. Lee SY, Bok KH, Kim JA, Kim C (2016) Simultaneous detection of Cu^{2+} and Cr^{3+} by a simple Schiff-base colorimetric chemosensor bearing NBD (7-nitrobenzo-2-oxa-1,3-diazolyl) and julolidine moieties. Tetrahedron 72:5563–5570

42. Jo HY, Lee SA, Na YJ, Kim C (2015) A colorimetric Schiff base chemosensor for CN^- by naked-eye in aqueous solution. Inorg Chem Commun 54:73–76

43. Lee JJ, Park GJ, Choi YW, Kim C (2015) Detection of multiple analytes (CN^- and F^-) based on a simple pyrazine-derived chemosensor in aqueous solution: experimental and theoretical approaches. Sensors Actuators B Chem 207:123–132

44. Puthiyedath T, Bahulayan D (2017) A click-generated triazole tethered oxazolone-pyrimidinone dyad: a highly selective colorimetric and ratiometric FRET based fluorescent probe for sensing azide ions. Sensors Actuators B Chem 239:1076–1086

45. Kawanishi Y, Kikuchi K, Takakusa H, Nagano T (2000) Design and Synthesis of intramolecular resonance-energy transfer probes for use in Ratiometric measurements in aqueous solution. Angew Chem 39:3438–3440

46. Becke AD (1993) Density-functional thermochemistry. III The Role of Exact Exchange J Chem Phys 98:5648–5652

47. Lee C, Yang W, Parr RG (1988) Development of the Colle-Salvetti correlation-energy formula into a functional of the electron density. Phys Rev B 37:785–789

48. M. J. Frisch, G. W. Trucks, H. B. Schlegel, G. E. Scuseria, M. A. Robb, J. R. Cheeseman, J. A. Montgomery Jr., T. Vreven, K. N. Kudin, J. C. Burant, J.M.Millam, S. S. Iyengar, J. Tomasi, V. Barone, B. Mennucci, M. Cossi, G. Scalmani, N. Rega, G. A. Peters CG and JAP (2004) GAUSSIAN 03 (revision B.02). Gaussian, Inc., Wallingford

49. Hariharan PC, Pople JA (1973) The influence of polarization functions on molecular orbital hydrogenation energies. Theor Chim Acta 28:213–222

50. Francl MM, Pietro WJ, Hehre WJ, Binkely JS, Gordon MS, Defrees DJ, Pople JA (1982) Self-consistent molecular orbital methods. 23. A polarization-type basis set for 2nd-row elements. J Chem Phys 77:3654–3665

51. Barone V, Cossi M (1998) Quantum calculation of molecular energies and energy gradients in solution by a conductor solvent model. J Phys Chem A 102:1995–2001

52. Cossi M, Barone V (2001) Time-dependent density functional theory for molecules in liquid solutions. J Chem Phys 115:4708–4717

53. O'Boyle NM, Tenderholt AL, Langner KM (2008) Cclib: a library for package-independent computational chemistry algorithms. J Comput Chem 29:839–845

54. Job P (1928) Formation and stability of inorganic complexes in solution. Ann Chim 9:113–203

55. Benesi HA, Hildebrand JH (1949) A spectrophotometric investigation of the interaction of iodine with aromatic hydrocarbons. J Am Chem Soc 71:2703–2707

56. Tsui Y-K, Devaraj S, Yen Y-P (2012) Azo dyes featuring with nitrobenzoxadiazole (NBD) unit: a new selective chromogenic and fluorogenic sensor for cyanide ion. Sensors Actuators B Chem 161:510–519